Human Molecular Genetics, 2010, Vol. 19, No. 10 ***1985–1997***
doi:10.1093/hmg/ddq077
Advance Access published on February 18, 2010

Uromodulin is expressed in renal primary cilia and *UMOD* mutations result in decreased ciliary uromodulin expression

Frank Zaucke[1], Joana M. Boehnlein[1], Sarah Steffens[1], Roman S. Polishchuk[4], Luca Rampoldi[5], Andreas Fischer[6], Andreas Pasch[7], Christoph W. A. Boehm[1], Anne Baasner[2], Massimo Attanasio[8,9], Bernd Hoppe[3], Helmut Hopfer[10], Bodo B. Beck[3], John A. Sayer[11], Friedhelm Hildebrandt[8,9] and Matthias T. F. Wolf[3,12,*]

[1]Center for Biochemistry, Medical Faculty, [2]Institute of Human Genetics and [3]Department of Pediatric Nephrology, University Children's Hospital, University of Cologne, Cologne, Germany, [4]Department of Cell Biology and Oncology, Consorzio 'Mario Negri Sud', Santa Maria Imbaro (CH), Italy, [5]Dulbecco Telethon Institute, DIBIT, San Raffaele Scientific Institute, Milan, Italy, [6]Department of Nephrology, Kantonsspital Lucerne, Lucerne, Switzerland, [7]Department of Nephrology and Hypertension, Inselspital, University of Berne, Berne, Switzerland, [8]Department of Pediatrics and [9]Department of Human Genetics, University of Michigan, Ann Arbor, MI, USA, [10]Department of Pathology, Universitätsspital Basel, Basel, Switzerland, [11]Institute of Human Genetics, Newcastle University, International Centre for Life, Newcastle upon Tyne NE1 3BZ, UK and [12]Pediatric Nephrology, Children's Medical Center, University of Texas Southwestern Medical Center, 5323 Harry Hines Blvd, Dallas, TX 75390-9063, USA

Received November 15, 2009; Revised January 20, 2010; Accepted February 17, 2010

***Uromodulin* (*UMOD*) mutations are responsible for three autosomal dominant tubulo-interstitial nephropathies including medullary cystic kidney disease type 2 (MCKD2), familial juvenile hyperuricemic nephropathy and glomerulocystic kidney disease. Symptoms include renal salt wasting, hyperuricemia, gout, hypertension and end-stage renal disease. MCKD is part of the 'nephronophthisis–MCKD complex', a group of cystic kidney diseases. Both disorders have an indistinguishable histology and renal cysts are observed in either. For most genes mutated in cystic kidney disease, their proteins are expressed in the primary cilia/basal body complex. We identified seven novel *UMOD* mutations and were interested if UMOD protein was expressed in the primary renal cilia of human renal biopsies and if mutant UMOD would show a different expression pattern compared with that seen in control individuals. We demonstrate that UMOD is expressed in the primary cilia of renal tubules, using immunofluorescent studies in human kidney biopsy samples. The number of UMOD-positive primary cilia in UMOD patients is significantly decreased when compared with control samples. Additional immunofluorescence studies confirm ciliary expression of UMOD in cell culture. Ciliary expression of UMOD is also confirmed by electron microscopy. UMOD localization at the mitotic spindle poles and colocalization with other ciliary proteins such as nephrocystin-1 and kinesin family member 3A is demonstrated. Our data add UMOD to the group of proteins expressed in primary cilia, where mutations of the gene lead to cystic kidney disease.**

INTRODUCTION

Uromodulin (*UMOD*) mutations have been reported in three autosomal dominant tubulo-interstitial nephropathies: (i) medullary cystic kidney disease (MCKD2) (OMIM 603860), (ii) familial juvenile hyperuricemic nephropathy (FJHN) (OMIM 162000) and (iii) in glomerulocystic kidney disease (GCKD) (OMIM 609886) (1–3).

*To whom correspondence should be addressed. Tel: +1 2146483438; Fax: +1 2146482034; Email: matthias.wolf@utsouthwestern.edu

UMOD mutations result in a urinary concentration defect, urinary salt wasting, hyperuricemia, gout, hypertension and end-stage renal disease (ESRD). MCKD2 is characterized by hypertension and ESRD in the fourth decade of life. Renal ultrasound in affected patients may show small corticomedullary cysts. MCKD2 shows a renal histologic triad of (1) tubular basement membrane disintegration (2), tubular atrophy with cyst development at the corticomedullary border and (3) interstitial cell infiltration associated with fibrosis. The condition shares clinical and morphological similarities with autosomal recessive juvenile nephronophthisis (NPHP) (4,5). In contrast to juvenile onset of ESRD and the autosomal-recessive inheritance in NPHP, MCKD2 leads to ESRD in adulthood and is inherited in an autosomal-dominant pattern (6). FJHN may present with hyperuricemia in childhood and early adult life (7). GCKD is characterized by a cystic dilatation of Bowman's space and a collapse of the glomerular tuft. Familial GCKD can be associated with hypoplastic kidneys (3). All three disorders show significant clinical overlap. Characteristics of both FJHN and MCKD2 were described in one kindred (8). Another group published 10 kindreds with *UMOD* mutations and FJHN. Five of the 10 kindreds had renal cysts and even within the same family there was variation with regard to the presence of cysts (2). Because all three phenotypes can be caused by the same *UMOD* mutation, these three disorders (FJHN, MCKD2 and GCKD) have also been described as 'Uromodulin-associated kidney disease' (UAKD) (9,10).

The *UMOD* gene encodes the Uromodulin (UMOD) protein (alias Tamm-Horsfall protein) and contains three epidermal growth factor-like (EGF-like) domains, a cysteine-rich D8C domain, and a zona pellucida domain. Forty-six different missense mutations in the *UMOD* gene have been described (1–3,11,12). For MCKD2, FJHN and GCKD patients, decreased urinary UMOD excretion and retention of the misfolded UMOD in the endoplasmatic reticulum (ER) is a postulated mechanism of disease (2,3,12). The mutant UMOD protein showed delayed ER to Golgi trafficking (12,13) as a result of an altered protein conformation and leading to an increased rate of apoptosis (14).

UMOD represents the most abundant urinary protein in humans (15). UMOD is expressed in renal tubular cells primarily at the apical surface of the thick ascending loop of Henle (TAL) and of the early distal convoluted tubules. It is a transmembrane protein, which is secreted into the urine through proteolytic cleavage of the glycosylphosphatidylinositol (GPI) anchor (16). UMOD is an 80–90 kDa macromolecule, which has been shown to be involved as a protective factor in urinary tract infections (UTI), in binding of complement factors and immunoglobulin light chains (to form casts in myeloma kidney), and as an inhibitor of nephrolithiasis (17–22). An *Umod* knock-out mouse model underlines the protective effects of UMOD in UTI caused by fimbriated *Escherichia coli* (23). Another mouse model ($UMOD^{A227T}$) shows that homozygous mice have a very similar phenotype to human UAKD with azotemia, impaired urine concentration and reduced urinary excretion of uric acid (24). In addition, a recent genome-wide association study found a significant single nucleotide polymorphism association of the *UMOD* locus with chronic kidney disease (25). Different modifications of the UMOD protein by N- and O-linked glycosylation have been described (26), and are responsible for interactions with interleukin-1, tumor necrosis factor-α, immunoglobulin light chains, IgG, complement 1 and 1q (20,21,27–29). Moreover stimulation of polymorphonuclear neutrophils, lymphocytes and monocytes by UMOD was shown (30–32). UMOD can directly activate dendritic cells via the Toll-like receptor 4 pathway, indicating a role in the innate immune response (33). In addition, the ability of UMOD to polymerize *in vitro* and so forming a gel-like structure has resulted in the hypothesis that UMOD is important for the water impermeability of the TAL (34).

Recently, ciliary expression of multiple 'cystoproteins', which are responsible for cystic kidney disease if altered, has been demonstrated (35). Expression in renal primary cilia was shown for: (i) polycystin-1 and -2, encoded by *PKD1* and *PKD2*, where mutations lead to autosomal-dominant polycystic kidney disease (ADPKD) (36); (ii) fibrocystin/polyductin, encoded by *PKHD1*, where mutations lead to autosomal-recessive polycystic kidney disease (ARPKD) (37); and (iii) the nephrocystin-1 to -11, proteins, where mutations in the genes *NPHP1-11* cause nephronophthisis (NPHP) (6). Ciliary and basal body expression was also shown for the protein products of Bardet–Biedl syndrome (BBS) genes. Patients with BBS and NPHP often share phenotypes (38). Ciliary expression has also been shown for the gene products of a number of cystic kidney knock-out mouse models implicating a role in the primary cilia for polaris, cystin, inversin and NEK8 (39–42). In addition, the transcription factor HNF1B was identified as an upstream regulator of nephrocystins and UMOD (43). In this report we describe seven novel mutations in the *UMOD* gene. Because of the previous hypothesis of the 'MCKD—nephronophthisis' complex, similar histopathological findings and the regulation of both genes by HNF1B, we were interested in studying: (i) if UMOD would be expressed in renal primary cilia, (ii) if mutant UMOD would show a different expression pattern and subcellular localization in human renal biopsies and (iii) if UMOD could be linked to the ciliary hypothesis of cystogenesis.

RESULTS

Mutation analysis

We performed mutational analysis in 54 individuals compatible with UAKD from 44 different unrelated kindreds. Out of the 54 individuals, 17 patients presented with familial disease in seven kindreds. Affected individuals underwent mutation analysis by exon polymerase chain reaction (PCR) and direct sequencing of all *UMOD* exons. We identified seven novel mutations in 11 individuals of seven kindreds: c.172 G > T (p.G58C); c.206G > A (p.C69Y); c.317G > A (p.C106Y); c.448T > A (p.C150S); c.688T > C (p.W230R); c.743G > C (p.C248S); c.821A > G (p.Y274C) (Table 1). In addition, we identified three previously published mutations in three individuals: 383del12/ins9 VCPEG93-97AASC; c.586G > A (p.D196N); c.898T > G (p.C300G) (Table 1). A cysteine residue was substituted by another amino acid in four of the seven novel *UMOD* mutations and in two of the previously known mutations. In two of the seven novel

Table 1. Summary of the identified *UMOD* mutations and corresponding patients' characteristics

Individual	Age at onset (years)	S. Cr. (mg/dl)	GFR (ml/min/1.73 m^2)	S. UA. (mg/dl)	Clinical characteristics	Ultrasound/biopsy findings	Mutation/(amino acid change)	PolyPhen PSIC score difference[a]	Affected *UMOD* domain
F1									
II-1	13	25.3	3	n.d.	anemia, ESRD, HTN, HD, proteinuria	US: ↑ echogenicity, renal atrophy, cysts	c.172 G > T (G58C)	2.397	EGF-like domain 1
II-2	12	3.3	23	n.d.	anemia	US: ↑ echogenicity, cysts, Bx: TIF, cysts, TA	c.172 G > T (G58C)	2.397	EGF-like domain 1
F2									
III-1	43	n.d.	n.d.	n.d.	ESRD, positive FHx[b]	Bx: sister with Bx	c.206G > A (C69Y)	3.084	EGF-like domain 2
F8									
II-1	49	2.8	n.d.	n.d.	HTN, ESRD, positive FHx[c]	Bx: TA, LPI, interstitial scarring	383del12/ins9 (VCPEG93-97AASC)[d]		EGF-like domain 2
F3									
II-1	50	n.d.	n.d.	n.d.	positive FHx[e]	MRI: brother with renal cysts and S.Cr. of 1.5	c.317G > A (C106Y)	3.185	EGF-like domain 2
F4									
I-1	27	2.0	61	7.0	HTN, anemia, hyperuricemia	US: nl, Bx: TA, LPI, TIF	c.448T > A (C150S)[f]	2.505	Cysteine-rich domain
II-1	23	n.d.	n.d.	n.d.	HTN, HD, NTX hyperuricemia	US: small atrophic kidneys B/L	c.448T > A (C150S)[f]	2.505	Cysteine-rich domain
F9									
II-1	n.d.	n.d.	n.d.	n.d.	n.d.	n.d.	c.586G > A (D196N)[d]		Cysteine-rich domain
F5									
II-1	36	2.5	37.5	12.6	gout, HTN, nocturia, positive FHx[g]	Bx: chronic interstitial nephritis	c.688T > C (W230R)	3.902	D8C
F6									
I-1	25	n.d.	n.d.	n.d.	CHF, HTN, ESRD, HD, gout, GI bleed, varices, aortic aneurysm	Bx: TA,TIF, thickened basement membrane anemia, HTN	c.743G > C (C248S)[h]	3.121	D8C
II-1	18	1.5	53	9.2			c.743G > C (C248S)[h]	3.121	D8C
II-2	18	2.2	58	n.d.	HTN, gout		c.743G > C (C248S)[h]	3.121	D8C
F7									
II-1	13	1.5	60	3.0	HTN, microhematuria, hearing, impairment, MR, positive FHx[i]	Bx: glomerulosclerosis, TA	c.821A > G (Y274C)	2.758	D8C
F10									
II-1	33	1.4	39.4	8.2	HTN, positive FHx[i]	n.d.	c.898T > G (C300G)[d]		D8C

B/L, bilateral; Bx: biopsy; CHF, congestive heart failure; ESRD, end-stage renal disease; GFR, glomerular filtration rate; HD, hemodialysis; HTN, hypertension; LPI, lympho-plasmacellular infiltrate; MR, mental retardation; MRI, magnetic resonance imaging; n.d., no data; nl, normal; NTX, renal transplant; S. Cr, serum creatinine; S. UA., serum uric acid; TA, tubular atrophy; TIF, tubulo-interstitial fibrosis; US, ultrasound.

[a]PolyPhen at http://genetics.bwh.harvard.edu/pph/index.html.

[b]FHx: The patient's mother (at the age of 54 years) and grandfather deceased because of ESRD. The patient's 1 year younger brother is treated with HD. The patient's 6 years younger sister has an elevated S.Cr. of 1.7 mg/dl. A renal US showed medullary cysts and increased echogenicity in her kidneys. A renal biopsy showed TIF, TA and nephrosclerosis.

[c]FHx: The patient's brother, paternal grandfather and uncle have a history of ESRD.

[d]Previously published mutation.

[e]FHx: A brother of the patient had an elevated serum creatinin of 1.5 mg/dl and an MRI showed bilateral renal cysts. The father of both patients required hemodialysis. DNA was only available from II-1.

[f]The same amino acid has been found previously affected by a c.449G > C (C150S) mutation (3).

[g]FHx: A sister has ESRD and gout. The patient's father died with advanced ESRD. No DNA was available from the father or the sister.

[h]The same amino acid has been found previously affected by a c.744C > G (C248W) mutation (10).

[i]FHx: Two brothers and a grandmother have been reported as affected. No DNA was available from these individuals.

[j]FHx: The patient's paternal grandmother and father suffer from ESRD. The father has also hypertension and gout.

UMOD mutations another amino acid was changed to a cysteine. None of the mutations were found in 100 healthy Caucasian controls, indicating that our detected mutations are unlikely to be common polymorphisms and are most likely disease-causing. Moreover, the PolyPhen software (http://genetics.bwh.harvard.edu/pph/index.html) predicted all

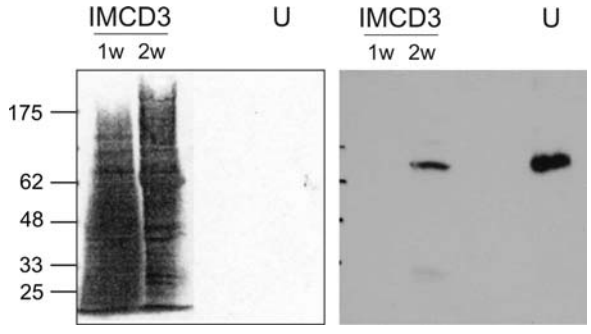

Figure 1. Analysis of the UMOD mouse antibody by western blot. Characterization of the UMOD mouse antibody. Cell lysates of IMCD3 cells were analyzed using 8% sodium dodecyl sulfate–polyacrylamide gel electrophoresis (SDS–PAGE) and probed with the mouse antibody for UMOD. The left panel shows the Ponceau staining of the western blot, demonstrating that similar protein concentrations were analyzed. The right blot demonstrates UMOD expression. The first and second lanes show cell lysates of IMCD3 cells, grown for 1 (1w) and 2 weeks (2w), respectively. In the very right lane, purified UMOD (U) was loaded as positive control. The molecular weight is shown at the left side in kilodaltons. The 2-week-old IMCD3 cell lysate and the urine UMOD show the expected size of 80 kDa for UMOD.

new mutations as probably damaging with significant position-specific independent counts (PSIC) score differences (Table 1). Mutations are mostly located in the EGF-like domains and the D8C domain.

Characterization of the UMOD mouse antibody in western blot and immunofluorescence staining of cell cultures

Prior to analysis of human kidney biopsies and cell cultures for possible primary cilia expression of UMOD, we characterized a primary UMOD antibody using western blots on cell lysates of IMCD3 cells. Lysates were separated on an 8% sodium dodecyl sulfate (SDS)–polyacrylamide gel electrophoresis (PAGE) and after electrotransfer, the membranes were probed with the mouse monoclonal antibody directed against UMOD. The IMCD3 lysates from different time points (Fig. 1, lanes 1 and 2) were compared with UMOD purified from urine (Fig. 1, lane 3, U). In cell lysates of post-confluent IMCD3 cells (which express primary cilia) grown for further 2 weeks, a clear band was detected by the UMOD antibody. This band had a molecular weight of 80 kDa as expected and migrated as the urinary UMOD. Staining of IMCD3 cells with the mouse antibody showed staining of the cytoplasm and the cilia. Primary cilia were visualized using an antibody directed against acetylated tubulin (Supplementary Material, Fig. S1). Pre-incubation of the antibodies with purified UMOD only reduced the staining for UMOD significantly but not for acetylated tubulin, thereby confirming specifity of the antibodies (Supplementary Material, Fig. S1).

In order to rule out any non-specific staining of the UMOD antibody to the cell surface or primary cilia, we treated IMCD3 cells with commercially available UMOD (up to 50 μg/ml) and repeated the UMOD antibody staining. No artificially increased UMOD staining was seen after the pre-incubation of cells with UMOD, indicating that the washing steps during the fixation and staining would remove non-specifically bound UMOD (data not shown). This experiment strongly suggests that the staining in renal tubules results from the expression of tubular cells rather than from urinary-free UMOD sticking non-specifically to the tubular surface.

Decreased UMOD expression in primary renal cilia of *UMOD* patients in human renal biopsies

In order to investigate the hypothesis that UAKD belongs to the group of diseases termed ciliopathies, we wanted to compare the number of UMOD-positive cilia in renal biopsy tissue from patients with known *UMOD* mutations versus control patient tissue.

In control experiments, we analyzed healthy renal biopsy tissue from four unaffected individuals for UMOD expression. We detected UMOD staining in ciliary structures pointing towards the tubular lumen (Fig. 2A). Co-staining with antibodies against acetylated tubulin confirmed that these structures are primary cilia (Fig. 2B). Two renal biopsies from patients with *UMOD* mutations were analyzed in detail. We anticipated a low number of patient biopsies, because a renal biopsy is not necessarily required for diagnosing UAKD.

Patient K11 (Fig. 2C and D) was diagnosed with a c.744C > G (C248W) mutation and her clinical characteristics have been extensively characterized (10). In summary, patient K11 is a female, who presented at the age of 46 years with a serum creatinine of 1.5 mg/dl, a glomerular filtration rate (GFR) of 58 ml/min/1.73 m^2 and a serum uric acid of 5.4 mg/dl. In addition, she had mild proteinuria and hypertension. A renal ultrasound showed four to five renal cysts bilaterally. A kidney biopsy revealed tubulo-interstitial sclerosis, fibrosis with interstitial lymphocytic cell infiltration, atrophic tubuli and a thickened basement membrane. After 6 years she required peritoneal dialysis. Patient F5 (Fig. 2E and F) was diagnosed with a novel c.688T > C (W230R) mutation, which was not present in 190 control individuals (Table 1). In order to rule out an unspecific effect reducing the ciliary UMOD staining owing to tubulo-interstitial kidney disease, we analyzed three kidney biopsies of patients with other tubulo-intersitial kidney diseases (Supplementary Material, Fig. S2). The three patients (C1–C3) were diagnosed with primary hyperoxaluria (C1) and interstitial nephritis (C2 and C3). In each renal biopsy specimen 20 tubules of the TAL, identified by intense UMOD staining, were analyzed for numbers of cilia and UMOD-positive cilia. In both of the UMOD patients' renal biopsies, we found a reduction in the total number of cilia in the TAL when compared with control samples (24 and 17 in 20 tubuli in each UMOD patient compared with the mean value of 44 in each of the four healthy control samples and 51 in each of the three patients with tubulo-interstitial kidney disease) (Table 2). About 86% of the primary cilia in the healthy control samples and 78% in the three patients with tubulo-intersitial kidney disease were UMOD-positive, while only 31% of cilia in UMOD patients were UMOD-positive (13 in two UMOD patients compared with 152 in the four healthy control samples and 119 in patients with tubulo-intersitial kidney disease) (Table 2). In patients with *UMOD* mutations, some primary cilia may still be found and appear morphologically normal, yet the total number of cilia and UMOD-positive

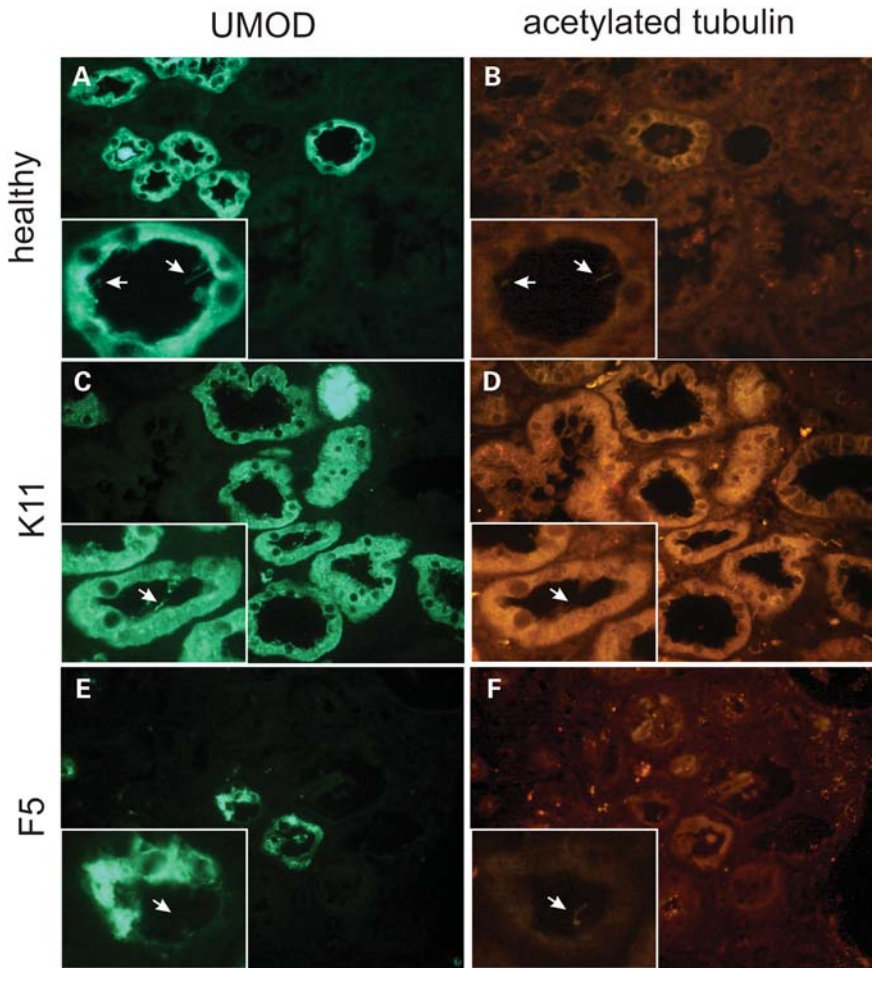

Figure 2. Ciliary UMOD expression in human renal biopsies. Renal samples from a human healthy control individual and two patients (K11 and F5) with *UMOD* mutations were stained for UMOD (A,C,E) and acetylated tubulin (B,D,F). In the healthy individuum and patient K11, hair-like structures were identified protruding into the tubular lumen of a TAL (arrows), indicating a UMOD stained cilium (**A,C**). Co-staining for acetylated tubulin detected exactly the same structures confirming ciliary expression of UMOD (**B,D**). In patient F5, a significant decrease of UMOD-positive tubulus was found. The staining pattern was irregular and the UMOD signal was not as uniformly distributed as in the control (**E**). There was a significant decrease in the total number of cilia detected by acetylated tubulin staining (**F**). In addition, the less abundant cilia were never co-stained for UMOD as indicated exemplarily by an arrow in (E) and (F).

cilia seems to be significantly lower than in the control samples.

Analysis of IMCD3 cell cultures for ciliary expression of UMOD by immunofluorescence

IMCD3 cells were grown on coverslips and maintained at confluence for 5 days before fixation in order to ensure maximal ciliary growth. Cells were then co-stained with antibodies directed against UMOD (Fig. 3A and D) and the ciliary marker acetylated tubulin (Fig. 3B and E). Images taken at lower magnification reveal that almost every cell expresses a single cilium at that time point. Colocalization of acetylated tubulin and UMOD was seen at the base and along the entire length of the cilium (Fig. 3C and F), indicating UMOD expression in the ciliary axoneme in IMCD3 cells. Higher magnification images show a punctate staining pattern (Fig. 3C′ and F′). These findings were confirmed by independent polyclonal antibodies against UMOD raised in goat (Fig. 3D–F and F′) and rabbit (data not shown). Colocalization of UMOD (Fig. 3G) and γ-tubulin (Fig. 3H) indicated UMOD expression in the basal bodies (Fig. 3I and I′). All negative controls, omitting primary antibodies and using secondary antibodies alone remained unstained (data not shown).

Analyzing UMOD expression in cilia by electron microscopy

In order to verify ciliary UMOD expression in IMCD3 cells, we performed immunogold labeling and electron microscopy (EM). Prior studies with EM have demonstrated impaired trafficking and retention of mutant UMOD in the ER (13). In post-confluent IMCD3 cells, UMOD was detected by immunogold labeling at the primary cilium, at the plasma membrane and in the ER (Fig. 4A). To prove further the point that our antibody is specific and is able to label UMOD inside the cells, we employed HeLa cells transfected with the C150S *UMOD* mutant. This mutant accumulates mainly within the ER, while it is almost absent at the plasma membrane (13). EM pictures clearly show specific labeling of the ER and nuclear

Table 2. Comparison of the numbers of cilia and UMOD-positive cilia in renal biopsies of four control individuals, two UMOD patients and three patients with other tubulo-interstitial kidney diseases (TIKD). Twenty tubules were analyzed in each individual

Sample	UMOD-positive cilia (%)	*P*-value[a]	No. of tubules analyzed
Control group ($n = 4$)	152/176 (86)		80
UMOD patients ($n = 2$)	13/41 (31)	0.0028	40
TIKD patients ($n = 3$)	119/152 (78)	0.565	60

[a]Fisher exact test determined two-tailed *P*-value.

envelop in transfected cells, while no labeling can be seen inside untransfected cells (Fig. 4B). This suggests that the antibody specifically labels intracellular structures when UMOD is present.

Mutant UMOD transfected IMCD3 cells show no UMOD ciliary expression

Examination of the renal tissue from two patients with *UMOD* mutations (K11 and F5) had revealed firstly a decrease in the total number of cilia and secondly a reduction in the number of UMOD-positive cilia when compared with controls (Fig. 2, Supplementary Material, Fig. S2, Table 2). In order to support our findings in human kidney biopsies, we transfected IMCD3 cells using previously described *UMOD* constructs, including two *UMOD* missense mutations (C150S, T225K) (13). We used an antibody directed against green fluorescent protein (GFP) to visualize exclusively transgenic UMOD protein (Fig. 5A). We found that in IMCD3 cells, the wild-type UMOD was trafficked normally and a typical cell surface staining was observed (Fig. 5A). In contrast, the *UMOD* mutation interferes with normal protein trafficking and intracellular protein aggregates were detected frequently (Fig. 5B). By co-staining with antibodies directed against GFP (Fig. 5C and D) and acetylated tubulin (Fig. 5E and F), we could show that transfected wild-type UMOD colocalizes partially with cilia (Fig. 5G), whereas mutant UMOD shows no ciliary expression (Fig. 5H). We were able to confirm our findings by using another *UMOD* mutation construct (T225K). The T225K *UMOD* mutation is known to result in a milder phenotype as the C150S *UMOD* mutation. The T225K mutation results in a better transport of UMOD protein to the plasma membrane compared with the C150S *UMOD* mutation (13). This is underlined by a more even and regular UMOD plasma membrane staining in the T225K UMOD transfected cells (Supplementary Material, Fig. S3). However, ciliary staining for UMOD is still absent (Supplementary Material, Fig. S3). This study confirms the ciliary expression and localization of UMOD using a second independent antibody for detection. Interestingly, expression of the C150S and T225K mutated UMOD resulted in an absence of UMOD ciliary expression, but did not necessarily lead to a loss of cilia (Fig. 5D, F and H).

Analysis of colocalization of UMOD, nephrocystin-1 and KIF3 in IMCD3 cells by immunofluorescence

In order to investigate whether UMOD colocalizes with other cystoproteins, IMCD3 cells were co-stained with antibodies directed against UMOD (Fig. 6A and D), nephrocystin-1 (Fig. 6B) and kinesin family member 3A (KIF3A) (Fig. 6E), respectively. Immunofluorescence showed a partial colocalization of UMOD with both nephrocystin-1 and KIF3A in cilia (Fig. 6C and F).

Analyzing UMOD expression in dividing IMCD3 cells

As nephrocystin-4 (alias nephroretinin), inversin (alias nephrocystin-2), nephrocystin-6 and RPGRIP1L (alias nephrocystin-8) were all shown to be expressed in the mitotic spindle poles (44–46), we were interested if UMOD would also be expressed at this position. Figure 7 shows staining of IMCD3 cells with polyclonal rabbit antibodies for UMOD (Fig. 7A) and acetylated tubulin (Fig. 7B). In mitotic cells, UMOD and acetylated tubulin colocalized at the spindle poles (Fig. 7C and C′) in a similar manner to nephrocystin-4 (nephroretinin) and inversin (44,47).

DISCUSSION

In patients with clinical evidence of UAKD, we found a total of seven new *UMOD* mutations in 11 individuals and confirmed three previously published mutations in another three individuals (Table 1). In our patient group, a cysteine residue was involved in six out of seven of the new mutations and in two out of the three known mutations. Cysteine is crucial for the formation of disulfide bridges and thus influences protein conformation. All new mutations were found in individuals with an autosomal-dominant pattern of renal disease. One patient (F7) had a more complex phenotype including mental retardation and hearing impairment. Five of the 11 patients had gout or hyperuricemia. All of our mutations are either missense mutations or deletions and occur in exons 4 or 5.

Patient F5's kidney biopsy appears more severely affected by the disease with significantly more tubular atrophy than patient K11. In comparison with patient K11, patient F5 had an earlier age of onset (36 versus 46 years), a lower GFR (37.5 versus 58 ml/min/1.73 m^2) and a higher serum creatinine (2.5 versus 1.5 mg/dl). Patient K11 had a severe clinical course and was started on peritoneal dialysis at 52 years. For patient F5, we do not have a significant follow-up period yet. Currently, patient F5 has chronic kidney disease stage 3 and no dialysis requirement.

By demonstrating an aberration in ciliary expression of UMOD, we suggest a novel pathophysiological mechanism for the etiology of MCKD2, FJHN and GCKD, by describing abberant ciliary expression of UMOD in patients with *UMOD* mutations. MCKD has previously been described to be part of the disease complex called 'nephronophthisis–MCKD complex' (4,5), given the fact that renal biopsies of patients with MCKD or nephronophthisis are indistinguishable. UMOD co-expression with nephrocystin-1 in the mitotic spindle and the decreased number of UMOD-positive cilia in

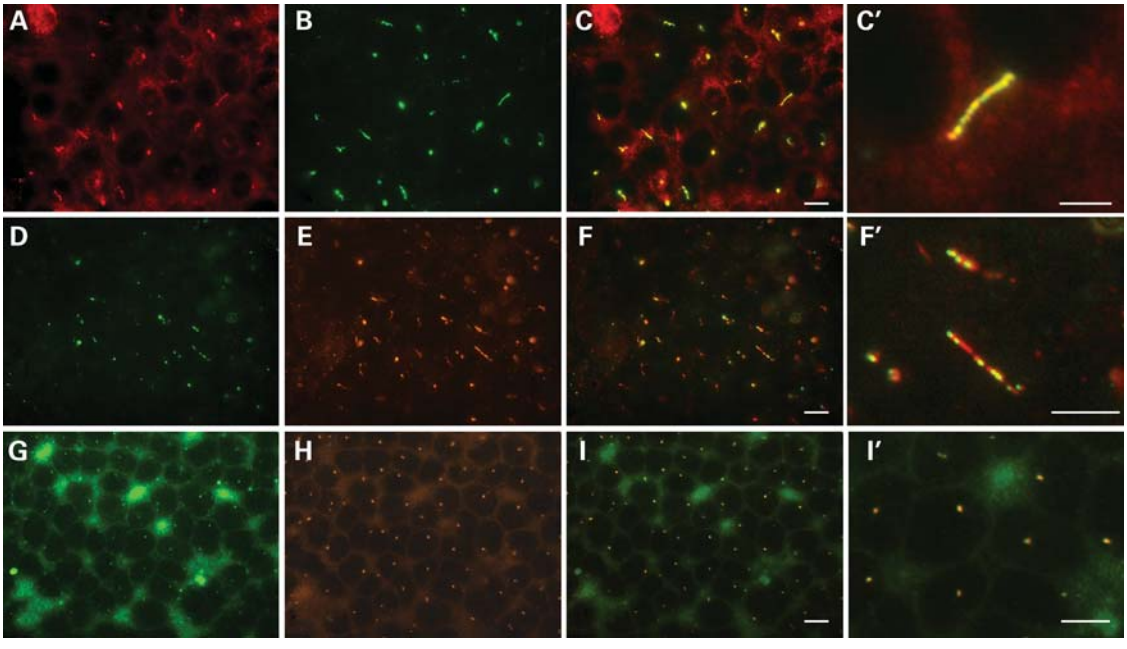

Figure 3. Immunofluorescence analysis of IMCD3 cell cultures for ciliary expression of UMOD. IMCD3 cells were stained with antibodies directed against UMOD (**A,D,G**) acetylated tubulin (**B,E**) and gamma tubulin (**H**). Co-staining of UMOD using two independent antibodies raised in mouse (**A**) and goat (**D**) with acetylated tubulin revealed an UMOD expression along the cilium (**C,F**). Higher magnifications show a punctate and not completely overlapping staining pattern (**C′,F′**). Co-staining of UMOD (**G**) and gamma tubulin (**H**) indicates the presence of UMOD also at the base of the cilium (**I,I′**). Merging these images shows colocalization of UMOD and γ-tubulin indicating expression of UMOD in basal bodies. All negative controls remained negative (data not shown). The scale bar represents 10 μm in (**C, F** and **I**) and 5 μm in (**C′, F′** and **I′**), respectively.

the kidney biopsies of UMOD patients suggests a specific function of UMOD in cilia. We showed that the reduced ciliary UMOD staining is specific for *UMOD* mutations and cannot be found in kidney biopsies of patients with other tubulo-interstitial kidney disorders (Supplementary Material, Fig. S2). Using transfection of wild-type and mutant *UMOD* constructs into IMCD3 cells, we reproduce the mislocalization defect for mutant UMOD in IMCD3 cells. The level of expression was similar for both constructs but the subcellular localization was clearly different (Fig. 5). We then analyzed the presence of cilia in transfected cells and could show that overexpressed wild-type UMOD could be detected in cilia. Expression of mutant UMOD showed absence of UMOD expression in primary cilia but did not result in a loss of cilia excluding a dominant-negative effect on cilia formation. Our findings suggest that there may be a common pathomechanism between these seperate genetic diseases, as their gene products colocalize to the same subcellular structures and suggest an involvement of UMOD in the nephrocystin multiprotein complex. There is significant overlap in the regulation and function of nephrocystins, polycystins, polyductin and UMOD, which supports our hypothesis. Firstly, a centrosomal localization was shown for nephrocystin-4, nephrocystin-6, RPGRIP1L/nephrocystin-8 and NEK8/nephrocystin-9 (44–46,48), while ciliary and basal body localization was demonstrated for nephrocystin-4 and RPGRIP1L/nephrocystin-8 (44,46). This corresponds to the same location where we identified UMOD by colocalization with γ-tubulin. Pyk2 and p130Cas have been shown to be part of the nephrocystin-1/nephrocystin-4 multiprotein complexes (44,49). A similar multiprotein complex was described for polycystin-1 and -2 with KIF3B (50). Even though colocalization does not necessarily mean that the proteins are active in the same pathway, we here show colocalization of UMOD with nephrocystin-1 and KIF3A, suggesting that UMOD may take part in such a multiprotein complex.

Secondly, it is interesting, that UMOD is also regulated by HNF1B, a transcription factor which also activates the nephrocystins and polycystins (43).

Moreover, sequence analysis has revealed ciliary localization sequences in polycystin-2 and G-protein-coupled receptors (51,52). A very short ciliary localization sequence shown for mouse somatostatin receptor 2 and 5 is shared by UMOD. This ciliary localization sequence encompasses the amino acids IRVG from position 448 to 451 and is located at the beginning of exon 8.

It is intriguing to speculate whether a secreted protein can play a role in planar orientation. Similar to UMOD, polyductin, which if altered causes ARPKD, is expressed in the primary cilium and is also secreted (53,54). The shed polyductin ectodomain and a concomitant C-terminal product, which is localized to the nucleus, may regulate the planar orientation of developing renal tubules in a paracrine fashion (53,54). This could imply that ciliary localized and secreted forms of proteins could have different functions.

Furthermore, ciliary function includes mechanosensation of urinary flow (55). It is speculated that the primary cilia sense the urine flow and thus provide vectorial information for orientated cell division (56). It is tempting to speculate that the protein expression in the TAL may be regulated by a mechano- or osmosensor, such as the primary cilium. Cilia are also involved in the canonical Wnt signaling pathway

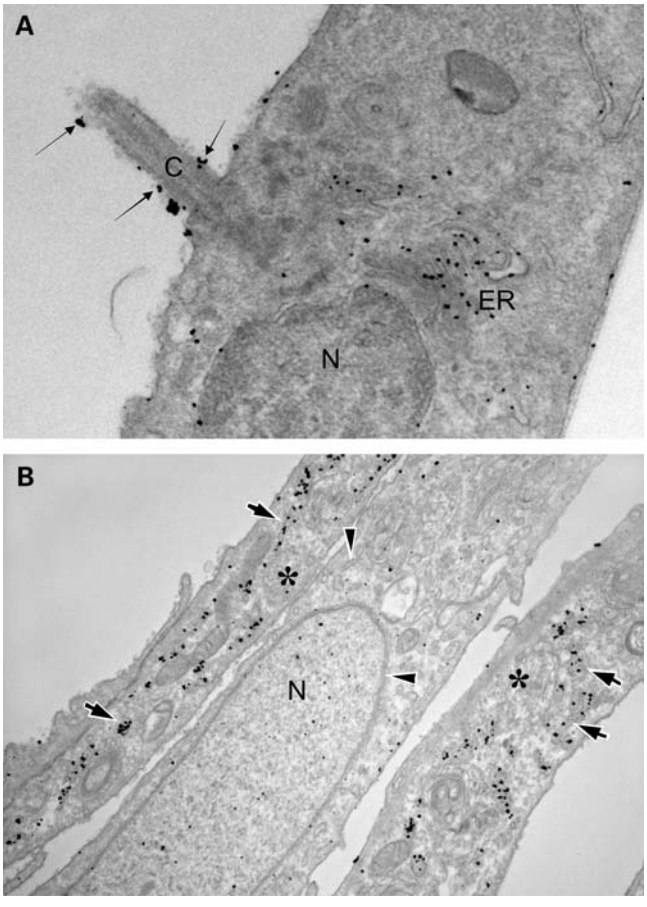

Figure 4. Analyzing UMOD expression in cilia by electron microscopy. (**A**) Endogenous ciliary UMOD expression in post-confluent IMCD3 cells was studied by electron microscopy. UMOD was detected by goldstaining in the ER, plasma membrane and at the cilium (arrows). (**B**) Positive and negative controls underlining the specifity of the immunogold UMOD antibody study. HeLa cells were transfected with the C150S *UMOD* mutant DNA. The C150S UMOD protein resides mainly within the ER (13). The upper and lower cells represent transfected cells (asterisks) with intense gold labeling along the ER membranes and nuclear envelop (arrows), while ER membranes and nuclear envelop (arrowheads) in the untransfected cell (in the middle) remain mostly devoid of gold particles. Untransfected HeLa cells do not express UMOD. Few randomly distributed particles that are visible inside untransfected cells were interpreted as background. ER, endoplasmic reticulum; N, nucleus; C, cilia.

(57). KIF3A has been shown to regulate the Wnt signaling pathway (58). The colocalization of KIF3A and UMOD could suggest that UMOD may be involved in the Wnt regulation also. Finally, cilia regulate cell cycle, cell proliferation and planar cell polarity. Nephrocystin-4 (44) and UMOD were also shown to be expressed in the mitotic spindle and defective proteins could cause either problems concerning the angle of the mitotic spindle or could cause dysfunction of the mitotic spindle, thus resulting in cyst formation.

Future studies will be required to address the specific role of UMOD in the context of the cilium.

The phenotypic variability in patients (MCKD2, FJHN, GCKD) with the same *UMOD* mutation and the previously known significant intrafamiliar differences in the phenotype have raised questions about additional contributing factors. We think that the conditional *Kif3a* knock-out mouse model (59) may improve our understanding with regard to phenotype variability. Adult conditional *Kif3a* knock-out mice did not develop cysts rapidly, despite a loss of primary cilia. However, acute kidney injury exacerbated cystic kidney disease underlining that *Kif3a* in primary cilia are required for the maintenance of planar cell polarity in the kidney (59). Only an additional trigger-like induction of acute renal injury, which resulted in increased cell proliferation, caused the development of renal cysts in mice (59).

Treatment of UMOD patients has been very challenging with contradictory reports about successful treatment with allopurinol and benzbromarone (7). Recently, inhibition of URAT1 by losartan was published (60), providing us with a new alternative medication for the treatment of hyperuricemia, which also addresses hypertension and proteinuria in UMOD patients.

Here, we present evidence that UMOD is ciliary and centrosomal expressed, implicating UMOD as a cystoprotein. We show that a decreased ciliary UMOD expression occurs following C150S, T225K (both in cell culture), W230R and C248W (both in kidney biopsies) *UMOD* mutations and may provide a pathophysiological mechanism contributing to this disease. We link UMOD to the ciliary network of proteins by colocalization with nephrocystin-1 and KIF3A. It is likely that UMOD is part of a multiprotein complex and takes part in the maintenance of cilia.

MATERIALS AND METHODS

Patients

We ascertained blood from 54 individuals from 44 different families who had a phenotype consistent with UAKD. Families are from Germany, Switzerland, the Netherlands, the UK and USA. Age at diagnosis, age at onset of ESRD, hyperuricemia, imaging data and biopsy results were reviewed if available. Diagnostic criteria were normal or small-sized kidneys with occasional small cortico-medullary cysts and renal insufficiency. At least one of the optional criteria as hypertension, a family history of renal disease, reduced fractional urinary excretion of uric acid or hyperuricemia was required. Hyperuricemia was defined as serum uric acid concentration >1 standard deviations higher than the normal values for age and gender (61). Renal biopsies from the UMOD patients were obtained where available. The kidney samples used as a control for UMOD expression were obtained from healthy poles of kidneys from nephrectomy specimens as part of the treatment for renal tumors. Additional control samples from patients with other tubulo-interstitial kidney disease were obtained from one patient with primary hyperoxaluria and two patients with interstitial nephritis. Samples were routinely fixed in 4% formaldehyde and embedded in paraffin. The study was approved by the institutional review board of the University of Cologne, Medical School. All participating family members provided informed consent.

Mutational analysis of the *UMOD* gene

Mutational analysis was performed by exon PCR of the *UMOD* gene. Primer sequences were used as described by

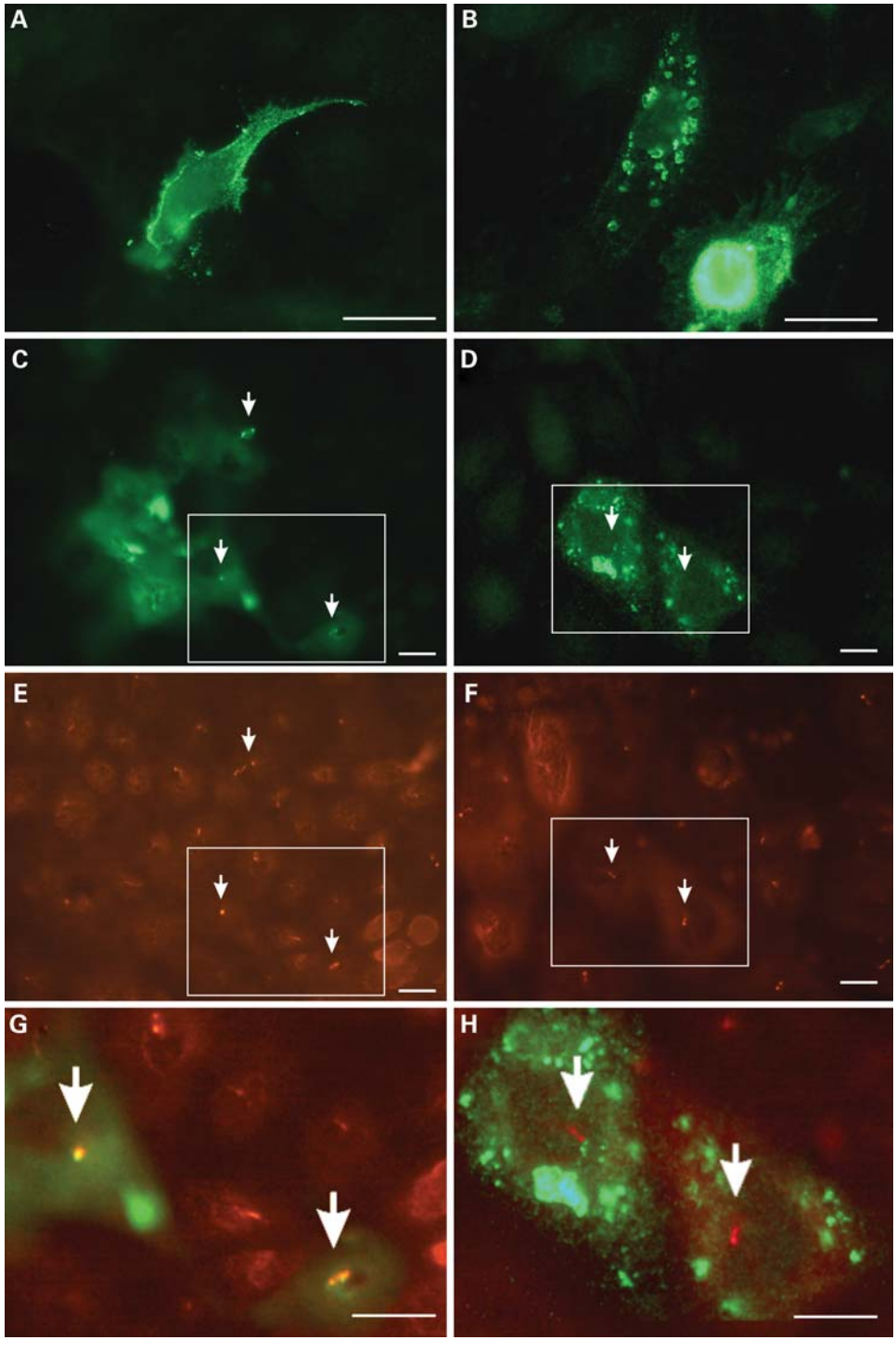

Figure 5. Overexpression of wild-type and mutant UMOD in IMCD3 cells. IMCD3 cells were transfected with wild-type (A,C,E,G) or C150S mutant UMOD–EGFP fusion constructs (B,D,F,H) and processed for immunofluorescence staining. Using an antibody directed against GFP, wild-type UMOD was mainly localized to the cell surface (**A**), while C150S mutant UMOD was detected mainly intracellularly in larger aggregates (**B**). A co-staining with antibodies directed against GFP and acetylated tubulin revealed ciliary expression for wild-type UMOD. Ciliary structures stained with both antibodies are indicated by arrows (**C,E,G**). In contrast, transfection with mutant *UMOD* did not result in ciliary UMOD localization (**D,H**). However, mutant *UMOD*-expressing cells still display cilia as indicated by arrows (**F**). A merge of the boxed areas in Figure 5C–F is shown in higher magnification (**G,H**). The scale bar represents 10 μm.

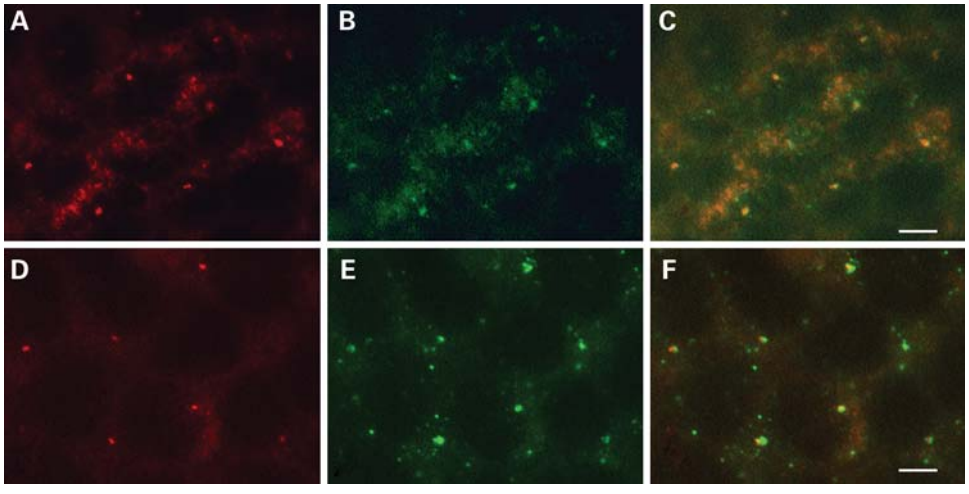

Figure 6. Colocalization of UMOD with nephrocystin-1 and KIF3A in cilia. IMCD3 cells were stained with antibodies directed against UMOD (**A,D**) nephrocystin-1 (**B**) and KIF3A (**E**). A merge of these stainings (**C,F**) demonstrate partial colocalization of UMOD with nephrocystin-1 and KIF3A. The scale bar in (C) and (F) represents 5 μm.

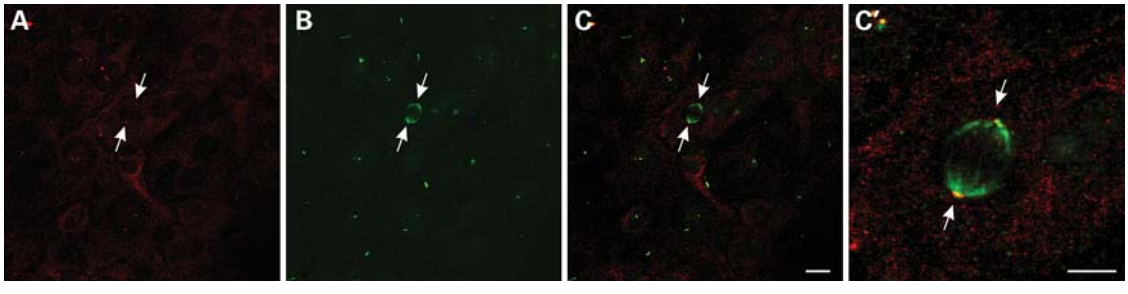

Figure 7. Detection of UMOD expression in the mitotic spindle poles. IMCD3 cell cultures were co-stained with antibodies directed against UMOD (**A**) and acetylated tubulin (**B**). In a mitotic cell, both signals colocalize in the spindle poles indicated by arrows (**C**). Higher magnification (**C′**). The scale bar in (C) and (C′) represent 10 and 5 μm, respectively.

Wolf *et al*. (11). PCR products were purified using the Marligen Rapid PCR Purification System. Purified PCR products were sequenced, using a Genetic Analyzer 3700 (Applied Biosystems) and resulting sequences were evaluated with the Sequencher™ software.

Cell culture and transfection

mIMCD3 cells were obtained from the American Type Culture Collection (www.atcc.org).

IMCD3 cells were maintained in DMEM/F12 media (Invitrogen) supplemented with 10% fetal calf serum, 2.5 mM L-glutamine, 15 mM HEPES, 0.5 mM sodium pyruvate, 1.2 g/l sodium bicarbonate. IMCD3 cells were transfected with Fugene (Roche) according to the manufacturer's instructions. The GFP-tagged wild-type and missense mutant (C150S, T225K) constructs have been described in detail (13).

SDS-PAGE and immunoblotting

Cell extracts were prepared by directly adding 2× SDS sample buffer (50 mM Tris–HCl, pH 6.8, 2% (w/v) SDS, 20% glycerol and 0.025% (w/v) bromphenol blue) to the cell layer. Samples were reduced (4% 2-mercaptoethanol, followed by 7 min heating at 95°C) and separated using 8% SDS–PAGE and transferred to nitrocellulose. After blocking, membranes were incubated either 1 h at room temperature (RT) or overnight at 4°C with primary antibodies (mouse monoclonal antibody against uromodulin, 1:500 dilution, Biozol, Eching, Germany), washed, incubated for 1 h at RT with a peroxidase-labeled antibody (Dako, Glostrup, Denmark), washed again and visualized with enhanced chemiluminescence. Specificity of the immunoblot was determined by co-migration with purified human uromodulin (Human Tamm Horsfall Glycoprotein, SCIPAC Ltd., Sittingbourne, UK) and diluted urine. In blocking experiments, the primary antibody directed against UMOD was preincubated overnight at 4°C with UMOD protein purified from urine.

Immunofluorescence

For immunofluorescence stainings, 20 000 cells were grown on glass chamber slides (Nalge Nunc Int., Rochester, NY, USA) for the indicated time after having reached confluency. Cells were fixed with 100% methanol for 10 min at −20°C, washed, blocked with 1% normal goat serum or 5% fetal calf serum and incubated with primary antibodies either for 2 h at RT or overnight at 4°C: mouse anti-human Tamm-Horsfall

protein (THP) monoclonal IgG2b (Biozol, Eching, Germany; dilution 1:500), goat anti-human THP polyclonal IgG (MP Biomedicals, Illkirch, France; dilution 1:100) or rabbit anti-human THP polyclonal IgG (Biotrend, Cologne, Germany; dilution 1:500) for UMOD detection; rabbit anti-nephrocystin-1 (NPHP1) polyclonal IgG (Biozol, Eching, Germany; dilution 1:100) and rabbit anti-KIF3A polyclonal IgG (Sigma, Saint Louis, USA; dilution 1:500) for spindle and plasma membrane localization; mouse anti-acetylated tubulin monoclonal IgG (Sigma, St Louis, USA; dilution 1:2000) and rabbit anti-acetylated tubulin polyclonal IgG (Biomol GmbH, Hamburg, Germany; dilution 1:500) for cilium detection; mouse anti-γ-tubulin monoclonal IgG (Sigma; dilution 1:300) for centrosome localization and anti-GFP rabbit polyclonal (Abcam, Cambridge, UK; dilution 1:500). For detection, fluorescence-labeled antibodies Alexa Fluor 488 goat anti-rabbit IgG, Alexa Fluor 488 donkey anti-goat IgG, Cy3 goat anti-mouse IgG, Cy3 donkey anti-rabbit IgG (Jackson Molecular Probes; dilution 1:1000) were used. For nuclear counterstaining, bisbenzimide (Sigma, Germany) was added to the cells for 3 min at a final concentration of 0.05 μg/ml. Slides were mounted in fluorescence mounting medium (DakoCytomation, Glostrup, Denmark) and analyzed by fluorescence (Axiophot, Zeiss) or confocal microscopy (Leica DMIRE 2). The blocking experiment was performed as described above. Paraffin-embedded tissue sections were processed using standard protocols and stained as described above.

Immuno-electron microscopy analysis

Post-confluent IMCD3 cells and transfected HeLa cells were fixed with a mixture of 4% paraformaldehyde and 0.05% glutaraldehyde 6–8 h after transfection, labelled with goat polyclonal primary antibody against uromodulin (ICN biomedicals) using the gold-enhance protocol, embedded in Epon-812 and cut as described previously (62). EM images were acquired from thin sections under a Philips Tecnai-12 electron microscope (Philips, Eindhoven, The Netherlands) using an ULTRA VIEW CCD digital camera.

SUPPLEMENTARY MATERIAL

Supplementary Material is available at *HMG* online.

ACKNOWLEDGEMENTS

We thank Dr B. Steiner and Professor Dr A. Schinzel from the University of Zurich, Switzerland; Dr C. Ferandos; Professor Dr H.P. Neumann from the University of Freiburg, Germany; Drs L. Pena and D. Waggoner from the University of Chicago, USA; and Dr M. Azar from the University of Texas, San Antonio, USA for sending us DNA from UAKD patients. We thank Dr Heike Göbel from the Institute of Pathology, University of Cologne, Germany, for making the kidney biopsy slides for the antibody staining experiments.

Conflict of Interest statement. None of the authors has a conflict of interest.

FUNDING

This work was supported by the Koeln Fortune Program Faculty of Medicine, University of Cologne (184/2004); Deutsche Nierenstiftung; and the German Research Foundation (DFG WO 1229/2-1) (for M.T.F.W.) and NIH (DK064614, DK069274 and DK068306) (for F.H.). J.A.S. is a GlaxoSmithKline clinician scientist. F.H. is a member of the Howard Hughes Medical Institute, a Doris Duke Distinguished Clinical Scientist and a F.G.L. Huetwell Professor. L.R. is financially supported by Telethon-Italy (Grant TCR08006) and through Coordination Theme 1 (Health) of the European Community's 7th Framework Program, EUNEFRON (GA number HEALTH-F2-2007-201590). L.R. is an Associate Telethon Scientist.

REFERENCES

1. Hart, T.C., Gorry, M.C., Hart, P.S., Woodard, A.S., Shihabi, Z., Sandhu, J., Shirts, B., Xu, L., Zhu, H., Barmada, M.M. *et al.* (2002) Mutations of the *UMOD* gene are responsible for medullary cystic kidney disease 2 and familial juvenile hyperuricaemic nephropathy. *J. Med. Genet.*, **39**, 882–892.
2. Dahan, K., Devuyst, O., Smaers, M., Vertommen, D., Loute, G., Poux, J.M., Viron, B., Jacquot, C., Gagnadoux, M.F., Chauveau, D. *et al.* (2003) A cluster of mutations in the *UMOD* gene causes familial juvenile hyperuricemic nephropathy with abnormal expression of *Uromodulin*. *J. Am. Soc. Nephrol.*, **14**, 2883–2893.
3. Rampoldi, L., Caridi, G., Santon, D., Boaretto, F., Bernascone, I., Lamorte, G., Tardanico, R., Dagnino, M., Colussi, G., Scolari, F. *et al.* (2003) Allelism of MCKD, FJHN, and GCKD caused by impairment of uromodulin export dynamics. *Hum. Mol. Genet.*, **12**, 3369–3384.
4. Waldherr, R., Lennert, T., Weber, H.P., Födisch, H.J. and Schärer, K. (1982) The nephronophthisis complex. A clinicopathologic study in children. *Virchows. Arch. A. Pathol. Anat. Histol.*, **394**, 235–254.
5. Hildebrandt, F. and Otto, E. (2000) Molecular genetics of nephronophthisis and medullary cystic kidney disease. *J. Am. Soc. Nephrol.*, **11**, 1753–1761.
6. Hildebrandt, F. and Zhou, W. (2007) Nephronophthisis-associated ciliopathies. *J. Am. Soc. Nephrol.*, **18**, 1855–1871.
7. McBride, M.B., Rigden, S., Haycock, G.B., Dalton, N., Van't Hoff, W., Rees, L., Raman, G.V., Moro, F., Ogg, C.S., Cameron, J.S. *et al.* (1998) Presymptomatic detection of familial juvenile hyperuricaemic nephropathy in children. *Pediatr. Nephrol.*, **12**, 357–364.
8. Bleyer, A.J., Woodard, A.S., Shihabi, Z., Sandhu, J., Zhu, H., Satko, S.G., Weller, N., Deterding, E., McBride, D., Gorry, M.C. *et al.* (2003) Clinical characterization of a family with a mutation in the uromodulin (Tamm-Horsfall glycoprotein) gene. *Kidney Int.*, **64**, 36–42.
9. Vylet'al, P., Kublová, M., Kalbácová, M., Hodanová, K., Baresová, V., Stibůrková, B., Sikora, J., Hůlková, H., Zivný, J., Majewski, J. *et al.* (2006) Alterations of uromodulin biology: a common denominator of the genetically heterogeneous FJHN/MCKD syndrome. *Kidney Int.*, **70**, 1155–1169.
10. Wolf, M.T., Beck, B.B., Zaucke, F., Kunze, A., Misselwitz, J., Ruley, J., Ronda, T., Fischer, A., Eifinger, F., Licht, C. *et al.* (2007) The *Uromodulin* C744G mutation causes MCKD2 and FJHN in children and adults and may be due to a possible founder effect. *Kidney Int.*, **71**, 574–581.
11. Wolf, M.T., Mucha, B.E., Attanasio, M., Zalewski, I., Karle, S.M., Neumann, H.P., Rahman, N., Bader, B., Baldamus, C.A., Otto, E. *et al.* (2003) Mutations of the *Uromodulin* gene in MCKD type 2 patients cluster in exon 4 which encodes three EGF-like domains. *Kidney Int.*, **64**, 1580–1587.
12. Williams, S.E., Reed, A.A., Galvanovskis, J., Antignac, C., Goodship, T., Karet, F.E., Kotanko, P., Lhotta, K., Morinière, V., Williams, P. *et al.* (2009) Uromodulin mutations causing familial juvenile hyperuricaemic nephropathy lead to protein maturation defects and retention in the endoplasmic reticulum. *Hum. Mol. Genet.*, **18**, 2963–2974.

13. Bernascone, I., Vavassori, S., Di Pentima, A., Santambrogio, S., Lamorte, G., Amoroso, A., Scolari, F., Ghiggeri, G.M., Casari, G., Polishchuk, R. *et al.* (2006) Defective intracellular trafficking of uromodulin mutant isoforms. *Traffic*, **7**, 1567–1579.
14. Choi, S.W., Ryu, O.H., Choi, S.J., Song, I.S., Bleyer, A.J. and Hart, T.C. (2005) Mutant tamm-horsfall glycoprotein accumulation in endoplasmic reticulum induces apoptosis reversed by colchicine and sodium 4-phenylbutyrate. *J. Am. Soc. Nephrol.*, **16**, 3006–3014.
15. Rindler, M.J., Naik, S.S., Li, N., Hoops, T.C. and Peraldi, M.N. (1990) Uromodulin (Tamm-Horsfall glycoprotein/uromucoid) is a phosphatidylinositol-linked membrane protein. *J. Biol. Chem.*, **265**, 20784–20789.
16. Santambrogio, S., Cattaneo, A., Bernascone, I., Schwend, T., Jovine, L., Bachi, A. and Rampoldi, L. (2008) Urinary uromodulin carries an intact ZP domain generated by a conserved C-terminal proteolytic cleavage. *Biochem. Biophys. Res. Commun.*, **370**, 410–413.
17. Tamm, I. and Horsfall, F.L. Jr. (1950) Characterization and separation of an inhibitor of viral hemagglutination present in urine. *Proc. Soc. Exp. Biol. Med.*, **74**, 106–108.
18. Pak, J., Pu, Y., Zhang, Z.T., Hasty, D.L. and Wu, X.R. (2001) Tamm-Horsfall protein binds to type 1 fimbriated *Escherichia coli* and prevents *E. coli* from binding to uroplakin Ia and Ib receptors. *J. Biol. Chem.*, **276**, 9924–9930.
19. Leeker, A., Kreft, B., Sandmann, J., Bates, J., Wasenauer, G., Múller, H., Sack, K. and Kumar, S. (1997) Tamm-Horsfall protein inhibits binding of S- and P- fimbriated *Escherichia coli* to human renal tubular epithelial cells. *Exp. Nephrol.*, **5**, 38–46.
20. Rhodes, D.C.J. (2002) Binding of Tamm-Horsfall protein to complement 1q and complement 1, including influence of hydrogen-ion concentration. *Immunol. Cell. Biol.*, **78**, 558–566.
21. Ying, W.Z. and Sanders, P.W. (2001) Mapping the binding domain of immunoglobulin light chains for Tamm-Horsfall protein. *Am. J. Pathol.*, **158**, 1859–1866.
22. Marengo, S.R., Chen, D.H., Kaung, H.L., Resnick, M.I. and Yang, L. (2002) Decreased renal expression of the putative calcium oxalate inhibitor Tamm-Horsfall protein in the ethylene glycol rat model of calcium oxalate urolithiasis. *J. Urol.*, **167**, 22192–22197.
23. Bates, J.M., Raffi, H.M., Prasadan, K., Mascarenhas, R., Laszik, Z., Maeda, N., Hultgren, S.J. and Kumar, S. (2004) Tamm-Horsfall protein knockout mice are more prone to urinary tract infection: rapid communication. *Kidney Int.*, **65**, 791–797.
24. Kemter, E., Rathkolb, B., Rozman, J., Hans, W., Schrewe, A., Landbrecht, C., Klaften, M., Ivandic, B.T., Fuchs, H., Gailus-Durner, V. *et al.* (2009) Novel missense mutation of uromodulin in mice causes renal dysfunction with alterations in urea handling, energy and bone metabolism. *Am. J. Physiol. Renal. Physiol.*, **297**, F1391–F1398.
25. Köttgen, A., Glazer, N.L., Dehghan, A., Hwang, S.J., Katz, R., Li, M., Yang, Q., Gudnason, V., Launer, L.J., Harris, T.B. *et al.* (2009) Multiple loci associated with indices of renal function and chronic kidney disease. *Nat. Genet.*, **41**, 712–717.
26. Wu, T.H., Hsieh, S.C., Yu, C.Y., Lee, Y.F., Tsai, C.Y. and Yu, C.L. (2008) Intact protein core structure is essential for protein-binding, mononuclear cell proliferating, and neutrophil phagocytosis-enhancing activities of normal human urinary Tamm-Horsfall glycoprotein. *Int. Immunopharmacol.*, **8**, 90–99.
27. Muchmore, A.V. and Decker, J.M. (1987) Evidence that recombinant IL 1 alpha exhibits lectin-like specificity and binds to homogeneous uromodulin via N-linked oligosaccharides. *J. Immunol.*, **138**, 2541–2546.
28. Sherblom, A.P., Decker, J.M. and Muchmore, A.V. (1988) The lectin-like interaction between recombinant tumor necrosis factor and uromodulin. *J. Biol. Chem.*, **263**, 5418–5424.
29. Rhodes, D.C., Hinsman, E.J. and Rhodes, J.A. (1993) Tamm-Horsfall glycoprotein binds IgG with high affinity. *Kidney Int.*, **44**, 1014–1021.
30. Thomas, D.B., Davies, M., Peters, J.R. and Williams, J.D. (1993) Tamm Horsfall protein binds to a single class of carbohydrate specific receptors on human neutrophils. *Kidney Int.*, **44**, 423–429.
31. Wimmer, T., Cohen, G., Saemann, M.D. and Hörl, W.H. (2004) Effects of Tamm-Horsfall protein on polymorphonuclear leukocyte function. *Nephrol. Dial. Transplant.*, **19**, 2192–2197.
32. Yu, C.L., Lin, W.M., Liao, T.S., Tsai, C.Y., Sun, K.H. and Chen, K.H. (1992) Tamm-Horsfall glycoprotein (THG) purified from normal human pregnancy urine increases phagocytosis, complement receptor expressions and arachidonic acid metabolism of polymorphonuclear neutrophils. *Immunopharmacology*, **24**, 181–190.
33. Säemann, M.D., Weichhart, T., Zeyda, M., Staffler, G., Schunn, M., Stuhlmeier, K.M., Sobanov, Y., Stulnig, T.M., Akira, S., von Gabain, A. *et al.* (2005) Tamm-Horsfall glycoprotein links innate immune cell activation with adaptive immunity via a Toll-like receptor-4-dependent mechanism. *J. Clin. Invest.*, **115**, 468–475.
34. Mattey, M. and Naftalin, L. (1992) Mechanoelectrical transduction, ion movement and water stasis in uromodulin. *Experientia*, **48**, 975–980.
35. Hildebrandt, F. and Otto, E. (2005) Cilia and centrosomes: a unifying pathogenic concept for cystic kidney disease? *Nat. Rev. Genet.*, **6**, 928–940.
36. Yoder, B.K., Hou, X. and Guay-Woodford, L.M. (2002) The polycystic kidney disease proteins, polycystin-1, polycystin-2, polaris, and cystin, are co-localized in renal cilia. *J. Am. Soc. Nephrol.*, **13**, 2508–2516.
37. Menezes, L.F., Cai, Y., Nagasawa, Y., Silva, A.M., Watkins, M.L., Da Silva, A.M., Somlo, S., Guay-Woodford, L.M., Germino, G.G. and Onuchic, L.F. (2004) Polyductin, the *PKHD1* gene product, comprises isoforms expressed in plasma membrane, primary cilium, and cytoplasm. *Kidney Int.*, **66**, 1345–1355.
38. Tobin, J.L. and Beales, P.L. (2007) Bardet-Biedl syndrome: beyond the cilium. *Pediatr. Nephrol.*, **22**, 926–936.
39. Brown, N.E. and Murcia, N.S. (2003) Delayed cystogenesis and increased ciliogenesis associated with the re-expression of polaris in Tg737 mutant mice. *Kidney Int.*, **63**, 1220–1229.
40. Hou, X., Mrug, M., Yoder, B.K., Lefkowitz, E.J., Kremmidiotis, G., D'Eustachio, P., Beier, D.R. and Guay-Woodford, L.M. (2002) Cystin, a novel cilia-associated protein, is disrupted in the cpk mouse model of polycystic kidney disease. *J. Clin. Invest.*, **109**, 533–540.
41. Morgan, D., Turnpenny, L., Goodship, J., Dai, W., Majumder, K., Matthews, L., Gardner, A., Schuster, G., Vien, L., Harrison, W. *et al.* (1998) Inversin, a novel gene in the vertebrate left-right axis pathway, is partially deleted in the inv mouse. *Nat. Genet.*, **20**, 149–156.
42. Liu, S., Lu, W., Obara, T., Kuida, S., Lehoczky, J., Dewar, K., Drummond, I.A. and Beier, D.R. (2002) A defect in a novel Nek-family kinase causes cystic kidney disease in the mouse and in zebrafish. *Development*, **129**, 5839–5846.
43. Gresh, L., Fischer, E., Reimann, A., Tanguy, M., Garbay, S., Shao, X., Hiesberger, T., Fiette, L., Igarashi, P., Yaniv, M. *et al.* (2004) A transcriptional network in polycystic kidney disease. *EMBO J.*, **23**, 1657–1668.
44. Mollet, G., Silbermann, F., Delous, M., Salomon, R., Antignac, C. and Saunier, S. (2005) Characterization of the nephrocystin/nephrocystin-4 complex and subcellular localization of nephrocystin-4 to primary cilia and centrosomes. *Hum. Mol. Genet.*, **14**, 645–656.
45. Sayer, J.A., Otto, E.A., O'Toole, J.F., Nurnberg, G., Kennedy, M.A., Becker, C., Hennies, H.C., Helou, J., Attanasio, M., Fausett, B.V. *et al.* (2006) The centrosomal protein nephrocystin-6 is mutated in Joubert syndrome and activates transcription factor *ATF4*. *Nat. Genet.*, **38**, 674–681.
46. Delous, M., Baala, L., Salomon, R., Laclef, C., Vierkotten, J., Tory, K., Golzio, C., Lacoste, T., Besse, L., Ozilou, C. *et al.* (2007) The ciliary gene *RPGRIP1L* is mutated in cerebello-oculo-renal syndrome (Joubert syndrome type B) and Meckel syndrome. *Nat. Genet.*, **39**, 875–881.
47. Morgan, D., Eley, L., Sayer, J., Strachan, T., Yates, L.M., Craighead, A.S. and Goodship, J.A. (2002) Expression analyses and interaction with the anaphase promoting complex protein Apc2 suggest a role for inversin in primary cilia and involvement in the cell cycle. *Hum. Mol. Genet.*, **11**, 3345–3350.
48. Otto, E.A., Trapp, M.L., Schultheiss, U.T., Helou, J., Quarmby, L.M. and Hildebrandt, F. (2008) *NEK8* mutations affect ciliary and centrosomal localization and may cause nephronophthisis. *J. Am. Soc. Nephrol.*, **19**, 587–592.
49. Benzing, T., Gerke, P., Höpker, K., Hildebrandt, F., Kim, E. and Walz, G. (2001) Nephrocystin interacts with Pyk2, p130(Cas), and tensin and triggers phosphorylation of Pyk2. *Proc. Natl Acad. Sci. USA.*, **98**, 9784–9789.
50. Wu, Y., Dai, X.Q., Li, Q., Chen, C.X., Mai, W., Hussain, Z., Long, W., Montalbetti, N., Li, G., Glynne, R. *et al.* (2006) Kinesin-2 mediates physical and functional interactions between polycystin-2 and fibrocystin. *Hum. Mol. Genet.*, **15**, 3280–3292.

51. Geng, L., Okuhara, D., Yu, Z., Tian, X., Cai, Y., Shibazaki, S. and Somlo, S. (2006) Polycystin-2 traffics to cilia independently of polycystin-1 by using an N-terminal RVxP motif. *J. Cell. Sci.*, **119**, 1383–1395.
52. Berbari, N.F., Johnson, A.D., Lewis, J.S., Askwith, C.C. and Mykytyn, K. (2008) Identification of ciliary localization sequences within the third intracellular loop of G-protein-coupled receptors. *Mol. Biol. Cell.*, **19**, 1540–1547.
53. Kaimori, J.Y., Nagasawa, Y., Menezes, L.F., Garcia-Gonzalez, M.A., Deng, J., Imai, E., Onuchic, L.F., Guay-Woodford, L.M. and Germino, G.G. (2007) Polyductin undergoes notch-like processing and regulated release from primary cilia. *Hum. Mol. Genet.*, **16**, 942–956.
54. Hiesberger, T., Gourley, E., Erickson, A., Koulen, P., Ward, C.J., Masyuk, T.V., Larusso, N.F., Harris, P.C. and Igarashi, P. (2006) Proteolytic cleavage and nuclear translocation of fibrocystin is regulated by intracellular Ca2+ and activation of protein kinase C. *J. Biol. Chem.*, **281**, 34357–34364.
55. Nauli, S.M., Alenghat, F.J., Luo, Y., Williams, E., Vassilev, P., Li, X., Elia, A.E., Lu, W., Brown, E.M., Quinn, S.J. *et al.* (2003) Polycystins 1 and 2 mediate mechanosensation in the primary cilium of kidney cells. *Nat. Genet.*, **33**, 129–137.
56. Fischer, E., Legue, E., Doyen, A., Nato, F., Nicolas, J.F., Torres, V., Yaniv, M. and Pontoglio, M. (2006) Defective planar cell polarity in polycystic kidney disease. *Nat. Genet.*, **38**, 21–53.
57. Simons, M., Gloy, J., Ganner, A., Bullerkotte, A., Bashkurov, M., Krönig, C., Schermer, B., Benzing, T., Cabello, O.A., Jenny, A. *et al.* (2005) Inversin, the gene product mutated in nephronophthisis type II, functions as a molecular switch between Wnt signaling pathways. *Nat. Genet.*, **37**, 537–543.
58. Corbit, K.C., Shyer, A.E., Dowdle, W.E., Gaulden, J., Singla, V., Chen, M.H., Chuang, P.T. and Reiter, J.F. (2008) Kif3a constrains beta-catenin-dependent Wnt signalling through dual ciliary and non-ciliary mechanisms. *Nat. Cell. Biol.*, **10**, 70–76.
59. Patel, V., Li, L., Cobo-Stark, P., Shao, X., Somlo, S., Lin, F. and Igarashi, P. (2008) Acute kidney injury and aberrant planar cell polarity induce cyst formation in mice lacking renal cilia. *Hum. Mol. Genet.*, **17**, 1578–1590.
60. Hamada, T., Ichida, K., Hosoyamada, M., Mizuta, E., Yanagihara, K., Sonoyama, K., Sugihara, S., Igawa, O., Hosoya, T., Ohtahara, A. *et al.* (2008) Uricosuric action of losartan via the inhibition of urate transporter 1 (URAT 1) in hypertensive patients. *Am. J. Hypertens.*, **21**, 1157–1162.
61. Wilcox, W.D. (1996) Abnormal serum uric acid levels in children. *J. Pediatr.*, **128**, 731–741.
62. Polishchuk, E.V., Di Pentima, A., Luini, A. and Polishchuk, R.S. (2003) Mechanism of constitutive export from the golgi: bulk flow via the formation, protrusion, and en bloc cleavage of large trans-golgi network tubular domains. *Mol. Biol. Cell.*, **14**, 4470–4485.